Quantification of Cerebral Arterial Blood Volume and Cerebral Blood Flow Using MRI With Modulation of Tissue and Vessel (MOTIVE) Signals

Tae Kim[1,2] and Seong-Gi Kim[1,3*]

Regional cerebral arterial blood volume (CBVa) and blood flow (CBF) can be quantitatively measured by modulation of tissue and vessel (MOTIVE) signals, enabling separation of tissue signal from blood. Tissue signal is selectively modulated using magnetization transfer (MT) effects. Blood signal is changed either by injection of a contrast agent or by arterial spin labeling (ASL). The measured blood volume represents CBVa because the contribution from venous blood was insignificant in our measurements. Both CBVa and CBF were quantified in isoflurane-anesthetized rats at 9.4T. CBVa obtained using a contrast agent was 1.1 ± 0.5 and 1.3 ± 0.6 ml/100 g tissue ($N = 10$) in the cortex and caudate putamen, respectively. The CBVa values determined from ASL data were 1.0 ± 0.3 ml/100 g ($N = 10$) in both the cortex and the caudate putamen. The match between CBVa values determined by both methods validates the MOTIVE approach. In ASL measurements, the overestimation in calculated CBF values increased with MT saturation levels due to the decreasing contribution from tissue signals, which was confirmed by the elimination of blood with a contrast agent. Using the MOTIVE approach, accurate CBF values can also be obtained. Magn Reson Med 54:333–342, 2005. © 2005 Wiley-Liss, Inc.

Key words: arterial blood volume; cerebral blood flow; arterial spin labeling; magnetization transfer effect; cerebral blood volume

Quantitative perfusion magnetic resonance imaging (MRI) has been widely used to investigate brain physiology because of the method's noninvasiveness and the ubiquity of MR scanners. Cerebral blood volume (CBV) has been measured by integrating MRI signals induced by the first pass of contrast agents after bolus injection (1), and cerebral blood flow (CBF) has been measured by means of arterial spin labeling (ASL) methods or by injecting contrast agents (2). CBF and CBV can be simultaneously measured by the continuous assessment of perfusion by tagging including volume and water extraction (CAPTIVE) method (3), which utilizes ASL with a specialized contrast agent (with causes a slight reduction of T_1) or by the double-echo flow-sensitive alternating inversion recovery (DEFAIR) method, which uses double-echo acquisitions at a range of inversion times (TIs) (4). However, the CAPTIVE method measures an index of relative CBV distributions, and the DEFAIR method has a low sensitivity and requires a long acquisition time. Both CBF and CBV are tightly regulated by arterial vessels, which have control mechanisms consisting of endothelial cells and smooth muscles. Thus, it is important to quantitatively measure cerebral arterial blood volume (CBVa). Duong and Kim (5) measured arterial blood volume using intravascular perfluorocarbon and ^{19}F NMR. Regional arterial and venous volume fractions can be resolved based on the fast- and slow-moving components in diffusion-weighted ^{19}F single-voxel spectra. Because of the limited sensitivity of the exogenous tracer, arterial blood volume cannot be obtained with high spatial resolution.

We propose to measure CBVa and CBF quantitatively using MRI techniques that rely on modulation of tissue and vessel (MOTIVE) signals. Signal intensity from the vessel pool can be changed by the injection of contrast agent or by ASL (6). A signal that originates from tissue can be selectively reduced by magnetization transfer (MT) effects (7,8). When protons in the tissue macromolecules are saturated by long RF pulse(s), their magnetization is transferred to tissue water protons (7,8). However, the signal from the blood pool is unaffected due to inflow of fresh spins from outside the coil's field of view (FOV) and minimal macromolecular blood content (7,8). With the application of graded MT saturation levels, signals that originate from tissue and vessel can be separated.

In ASL methods, the measured CBF values may be overestimated due to contamination of blood signals. To measure CBF accurately, signals of only tissue and capillaries should be measured, while signals from large vessels should be minimized. Especially in continuous ASL (CASL) measurements with one homogeneous coil, tissue signals decrease due to significant MT effects, accentuating the relative contribution of arterial blood signal. With graded MT saturation levels in ASL measurements, without changing ASL efficiency the effect of CBVa on calculated CBF values can be examined.

In this study, detailed relaxation mechanisms were used to measure CBVa. Arterial blood volumes of rat brains were measured by two different approaches: injection of a contrast agent, and ASL. Then the consistency of the CBVa values measured by these two different methods was examined. Also, CBF values at different MT saturation levels were determined and compared with those obtained with the suppression of blood signals using contrast agent.

[1]Department of Neurobiology, University of Pittsburgh, Pittsburgh, Pennsylvania, USA.

[2]Center for Magnetic Resonance Research, University of Minnesota, Minneapolis, Minnesota, USA.

[3]Department of Radiology, University of Pittsburgh, Pittsburgh, Pennsylvania, USA.

Grant sponsor: NIH; Grant numbers: EE03375; EB03324; NS44589; EB01977; RR08079.

*Correspondence to: Seong-Gi Kim, Ph.D., Department of Neurobiology, University of Pittsburgh Medical School, 3025 East Carson Street, Pittsburgh, PA 15203. E-mail: kimsg@ pitt.edu

Received 22 July 2004; revised 18 February 2005; accepted 18 February 2005.

DOI 10.1002/mrm.20550
Published online in Wiley InterScience (www.interscience.wiley.com).

THEORY

It is assumed that MRI signals in a given pixel originate from three compartments: tissue, arterial blood, and venous blood. The total blood volume measured by positron emission tomography (PET) is 4–5% in both rhesus monkeys (9) and humans (10). According to arterial and venous blood volume measurements with ^{19}F NMR in rats, the arterial volume fraction is ~30% of total blood volume (5). A volume fraction of the arterial compartment is 1–2% of the total volume, the venous compartment is 3–4%, and the remaining volume corresponds to the tissue pool (5,9,10). At 9.4T, T_2 of tissue and arterial blood is 40 ms, while T_2 of venous blood is 5–7 ms (11). When the TE is >3 times the T_2 value of venous blood, signal intensity from the venous blood pool will be negligible, and thus the remaining signals represent tissue and arterial blood. The tissue pool is defined to include tissue and capillary blood volume. On a T_1 time scale (i.e., spin labeling time > 2 s), water in capillaries freely exchange with tissue water in respect to an exchange time of water (~500 ms) (12). Thus, tissues and capillaries are not separable for longitudinal magnetization during a spin preparation period.

At a steady-state condition with the MT effect, the signal intensity at an appropriate spin echo time (TE), S_{sat} can be written as

$$S_{sat} \cong (1 - \nu_a - \nu_v)M_{sat} \cdot e^{-R_{2(tissue)} \cdot TE} + \nu_a \cdot M_0 \cdot e^{-R_{2(artery)} \cdot TE} \quad [1]$$

where ν_a and ν_v are the fraction of spins in arterial and venous pools (not physical volume), respectively; R_2 is the transverse relaxation rate at the corresponding compartment (tissue and artery); M_{sat} is the saturated tissue magnetization with the various MT effect, and M_0 is the fully relaxed magnetization. In the case of no MT effect, $M_{sat} = M_0$. When gradient-echo data collection is used, R_2 should be replaced by R_2^* throughout all equations. It should be noted that tissue and blood have different spin densities. Since, ν_a is the fraction of spins in arterial blood pool (a unit of %), a change in spin density will change ν_a. To convert from spin fraction ν_a into physical volume CBVa, differences in spin density between tissue and blood pools must be considered. Thus, CBVa will be $\nu_a \times \lambda$ where λ is the blood–brain partition coefficient (ml blood/g tissue).

To separately measure tissue (i.e., the first term in Eq. [1]) and blood (i.e., the second term in Eq. [1]) contributions, it is preferable to use MOTIVE signals. Tissue signal can be selectively modulated by various MT saturation levels while blood signal can be changed by injection of intravascular contrast agent or by ASL. The theoretical bases of both approaches are given below.

MOTIVE Approach With Contrast Agent: Measurements of Arterial Blood Volume

When a blood pool contrast agent, such as monocrystalline iron oxide nanoparticle (MION), is injected into blood, the R_2 values (and R_2^*) of blood and tissue are increased. After the injection of contrast agents, the measured signal intensity S_{sat}^{MION}, with graded MT saturation levels modulated by different RF power levels, is similar to Eq. [1] with additional signal decay terms induced by MION as

$$S_{sat}^{MION} = (1 - \nu_a - \nu_v)M_{sat} \cdot e^{-(R_{2(tissue)} + \Delta R_{2(tissue)}) \cdot TE} + \nu_a \cdot M_0 \cdot e^{-(R_{2(artery)} + \Delta R_{2(blood)}) \cdot TE} \quad [2]$$

where $\Delta R_{2(tissue)}$ and $\Delta R_{2(blood)}$ are the R_2 change in tissue and blood induced by MION, respectively. By combining Eqs. [1] and [2], M_{sat} can be removed. Normalized signal intensities of images with MT effects after the injection of MION S_{sat}^{MION}/S_o can be described as

$$S_{sat}^{MION}/S_o = S_{sat}/S_o \cdot e^{-\Delta R_{2(tissue)} \cdot TE} + \nu_a \cdot M_0 \cdot e^{-R_{2(artery)} \cdot TE}(e^{-\Delta R_{2(blood)} \cdot TE} - e^{-\Delta R_{2(tissue)} TE})/S_o \quad [3]$$

where $S_o = [(1 - \nu_a - \nu_v) \cdot e^{-R_{2(tissue)} \cdot TE} + \nu_a \cdot e^{-R_{2(artery)} \cdot TE}]M_o$, obtained without MT effects before the injection of contrast agents. Since the R_2 values of tissue and arterial blood are similar at 9.4T, $M_o e^{-R_{2(artery)} \cdot TE}$ in the second term is canceled out. The resulting denominator in the second term, $1 - \nu_v$, is approximated to 1.0, and Eq. [3] can be rewritten as

$$S_{sat}^{MION}/S_o = S_{sat}/S_o \cdot e^{-\Delta R_{2(tissue)} \cdot TE} + \nu_a \cdot (e^{-\Delta R_{2(blood)} \cdot TE} - e^{-\Delta R_{2(tissue)} TE}) \quad [4]$$

$\Delta R_{2(tissue)}$ will be determined by the slope of linear fitting to the normalized signal intensities with different MT saturation levels before and after the injection of contrast agents. $\Delta R_{2(blood)}$ can be measured from withdrawn arterial blood. Since the intercept = $\nu_a \cdot (e^{-\Delta R_{2(blood)} TE} -$ slope), ν_a is calculated from the intercept, the slope, and $\Delta R_{2(blood)}$.

MOTIVE Approach With ASL: Measurements of Arterial Blood Volume and CBF

ASL can be achieved by continuously perturbing spins within the carotid arteries. In most perfusion studies (2,13,14), *suppression* of the arterial blood signal (for instance, by means of flow-crushing gradients) has been of major interest in the effort to obtain accurate CBF values. In our studies, arterial blood and tissue components were discriminated using MT effects with a constant ASL efficiency α. When ASL is achieved, a change in blood magnetization is $2\alpha \cdot M_0$ and a change in tissue magnetization is $C \cdot M_{sat}$ where C is a constant related to tissue perfusion, which is $2\alpha \frac{f}{\lambda} \Big/ \left(\frac{1}{T_1} + \frac{f}{\lambda}\right)$, where f is CBF (ml/100 g tissue/min), T_1 is T_1 of tissue without MT effects, and λ is the blood–brain partition coefficient (15,16). It should be noted that the water extraction fraction was assumed here to be 1.0. The difference signal between nonlabeled control and labeled images ΔS_{sat} can be expressed as

$$\Delta S_{sat} = (1 - \nu_a - \nu_v) \cdot C \cdot M_{sat} e^{-R_{2(tissue)} \cdot TE} + \nu_a \cdot 2\alpha \cdot M_o e^{-R_{2(artery)} \cdot TE} \quad [5]$$

Then M_{sat} is replaced using Eq. [1]. The normalized difference signal, $\Delta S_{sat}/S_o$ can be written as

$$\Delta S_{sat}/S_o = C\cdot(S_{sat}/S_o) + \nu_a(2\alpha - C)M_o e^{-R_{2(artery)}\cdot TE}/S_o$$
$$= C\cdot(S_{sat}/S_o) + \nu_a(2\alpha - C) \quad [6]$$

By fitting a linear function to $\Delta S_{sat}/S_0$ vs. S_{sat}/S_0, the slope and intercept can be calculated. Since the intercept = $\nu_a \cdot (2\alpha - \text{Slope})$, ν_a can be calculated from the intercept, slope, and α. If the calculation of CBVa is accurate, ν_a should be same whether arterial blood signal is modulated by contrast agent (Eq. [4]) or by ASL (Eq. [6]).

The CBF can be directly determined from the slope C in Eq. [6] without any arterial blood volume contribution as

$$\text{CBF} = \frac{\lambda}{T_1}\left(\frac{C}{2\alpha_c - C}\right) \quad [7]$$

The spin tagging efficiency is considered by T_1 relaxation of labeled spins during travel from the labeling plane to the *exchange site* in capillaries. Here, $\alpha_c = \alpha_o \cdot e^{-(\tau_c \cdot R_{1b})}$ where α_o is the degree of labeling efficiency at the carotid arteries in the neck, τ_c is the transit time of labeled spins from the labeling plane into the exchange site at the brain, and R_{1b} is the R_1 of arterial blood.

Alternatively, CBF values can be also determined using a conventional, freely diffusible, one-compartment model (17) as

$$\text{CBF} = \frac{\lambda}{T_1}\left(\frac{\Delta S_{sat}}{2\alpha\cdot S_{sat} - \Delta S_{sat}}\right) \quad [8]$$

where α is the spin tagging efficiency. CBF determined by Eq. [8] may be overestimated by the contribution of arterial blood signal. If ΔS_{sat} contains arterial blood signals, $\alpha = \alpha_o \cdot e^{-(\tau_a \cdot R_{1b})}$, where τ_a is the transit time of labeled spins from the labeling plane to the imaging slice. If ΔS_{sat} does not have the arterial vessel component (i.e., $C = \Delta S_{sat}/S_{sat}$), $\alpha = \alpha_c$, and Eqs. [7] and [8] are the same. CBF values can be calculated from each pair of control and labeled images with the MT saturation level using Eq. [8], while a CBF value is determined from all pairs of images with various MT saturation levels using Eq. [7].

MATERIALS AND METHODS

Animal Preparation

All animal protocols were approved by the University of Minnesota Animal Care and Use Committee. Male Sprague-Dawley rats weighing 300–350 g (Charles River Laboratories, Wilmington, MA, USA) were initially anesthetized with 5% isoflurane in a mixture of O_2 and N_2O gases, and intubated for ventilation. Once the animals were fully anesthetized, the isoflurane level was maintained at 1.5%, with O_2:N_2O of 1:2 throughout the experiments. Two femoral arteries were catheterized for blood pressure monitoring and blood gas sampling, and one femoral vein was catheterized for fluid administration and injection of contrast agent. The arterial blood pressure and the breathing pattern were recorded with a multitrace recorder (AcKnowledge; Biopak, CA, USA) throughout the experiments. Blood gas was sampled intermittently and maintained at physiological levels (pH = 7.35–7.45, pCO_2 = 35–45 mmHg, pO_2 = 120–200 mmHg, and mean blood pressure = 100–130 mmHg). The head of the animal was carefully secured in an in-house-made stereotaxic frame with ear pieces and a bite bar. The animal's rectal temperature was maintained at 37°C ± 1°C by means of a warm circulating-water pad, rectal thermocoupled probe, and feedback unit. At the end of the experiments, the animals were killed by an overdose of KCl while they were under deep anesthesia.

MRI Methods

All of the MRI measurements were performed on a 9.4T, 31-cm-diameter bore horizontal magnet (Magnex, Abingdon, UK) interfaced to a Unity INOVA console (Varian, Palo Alto, CA, USA). The system was equipped with an actively shielded 11-cm inner diameter gradient insert (Magnex, Abingdon, UK). For the ASL experiments, an actively detunable two-coil system was used. It consisted of a butterfly-shaped surface coil that was positioned in the neck region, and a surface coil (2.3 cm diameter) that was positioned on top of the rat head for imaging. Since actively decoupled switching coils were used, spin labeling pulses did not generate significant MT effects in the brain, and consequently no asymmetric MT effects between the two images were observed, which was confirmed experimentally. The homogeneity of the magnetic field was manually optimized on a slab that was twice as thick as the imaging slice.

Single-slice, 2-mm-thick coronal images were acquired using an adiabatic single-shot double spin echo-planar imaging (EPI) sequence with TE = 25 ms, TR = 10 s, matrix size = 64 (readout direction) × 32 (phase-encoding direction), and FOV = 3.0 (right–left hemisphere direction) × 1.5 (dorsal–ventral direction) cm^2 to obtain B_1-insensitive accurate flip angles. T_1 of tissue water proton was measured with the use of an inversion recovery EPI sequence. A recovery time of 10 s was allowed before the next adiabatic inversion pulse was applied. Logarithmically spaced TIs (0.14, 0.28, 0.45, 0.62, 0.81, 1.02, 1.25, 1.52, 1.83, 2.2, 2.64, 3.21, 4.02, 5.41, 6, 7, 8, and 9.0 s) were used in a randomized order.

To modulate a level of MT effects without changing ASL efficiency, we used two actively-detunable surface coils: one to generate ASL in the carotid arteries in the neck, and one to generate MT effects in the brain and collect images. A pair of pulses (a 100-ms spin tagging pulse in the neck coil, followed by a 100-ms MT-inducing pulse in the head coil) was repeated during a spin preparation period (see Fig. 1).

CBVa was measured by two MOTIVE approaches in the same animal. Both methods relied on a graded MT saturation level. To generate various MT saturation levels in the brain using the head coil with actively detuning the neck coil, five power levels of RF pulses with +8500 Hz offresonance frequency were used in a randomized order. A steady-state condition was achieved without spin labeling in the cortex up to ~30% of the signal intensity without any MT effect, and the signal decreased by ~70%. The duration of the MT preparation was varied up to 8.0 s to achieve a steady-state condition.

The blood signal can be modulated by injection of contrast agent or ASL. To measure CBVa using the MOTIVE

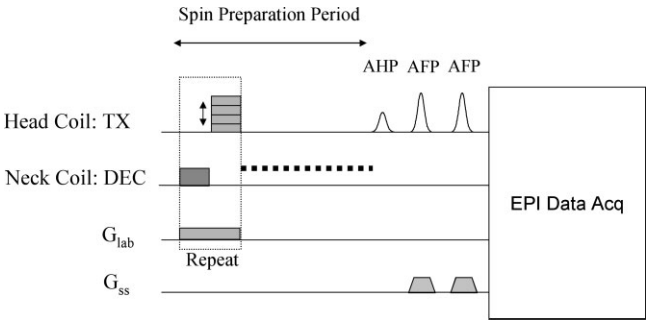

FIG. 1. Diagram of an ASL pulse sequence with variable MT effects. Two actively decoupled coils were used to utilize this pulse sequence: a neck coil connected to a decoupling channel (DEC) was used to label arterial spins, and a head coil connected to a transmitter channel (TX) was used to obtain images and generate MT effects. A pair of pulses (a 100-ms spin tagging pulse in the neck coil, followed by a 100-ms MT-inducing pulse in the head coil) were repeated during a spin preparation period. To generate different MT saturation levels, the RF power level for MT-generating pulses was adjusted without changing the spin labeling efficiency. Single-shot, double spin-echo EPI was used for data collection. A non-slice-selective adiabatic half passage (AHP) RF pulse was used for spin excitation, and two slice-selective adiabatic full passage (AFP) RF refocusing pulses were applied. Both adiabatic pulses are based on sech amplitude and tanh frequency modulation functions. G_{lab}: *z*-axis gradient of 10 mT/m; G_{ss}: slice-selection gradient.

approach with a contrast agent, modulation of MT saturation levels was performed in the same animal before and after the injection of 1 mg Fe/kg MION contrast agent. To determine CBVa with ASL in the MOTIVE method, ASL with a graded MT saturation level was performed. To determine signal changes induced by ASL, control and spin-labeled images were obtained in an interleaved manner. The labeling frequency was about −8500 Hz (with a field gradient strength of 10 mT/m), while the control frequency was about +8500 Hz with respect to the resonance frequency. After the injection of 1 mg Fe/kg MION, the same ASL experiment was performed to determine the effect of blood contribution to CBF quantification. ASL efficiency at the carotid arteries α_o was determined before and after the injection of MION using an 8-s continuous spin labeling pulse (17).

To determine $\Delta R_{1(\mathrm{blood})}$ and $\Delta R_{2(\mathrm{blood})}$ induced by MION, 1.0 ml of arterial blood was drawn into heparinized syringes before and after the injection of MION. Whole blood was used for T_2 measurements. The blood was centrifuged and the plasma was extracted to minimize precipitation of red blood cells during T_1 measurements. T_1- and T_2-weighted spectra of blood were obtained at room temperature using conventional inversion-recovery and spin-echo spectroscopic methods, respectively. T_1 and T_2 were calculated with single-exponential fitting of spectral peak heights using VNMR software (Varian).

Data Analysis

To improve the SNRs, 10–15 repeated measurements were averaged before further analysis was performed. All data were normalized by the images obtained without any MT effect before MION injection (S_0). For pixel-by-pixel analysis, a 2D Gaussian filter with the standard deviation (SD) of the distribution ($\sigma = 0.85$) and a kernel size of 3×3 was applied to reduce noise. For a quantitative comparison between measurements, three regions of interest (ROI) were chosen in the cerebral cortex, the caudate-putamen, and the middle internal artery (marked as CTX, CPU, and A, respectively), based on anatomic images (Fig. 2a). Signals from pixels within the ROIs were averaged before the data were fit to a linear function. The CBVa values were determined using Eqs. [4] and [6], with $\lambda = 0.9$ ml/g. The CBVa values of each animal, obtained by the two approaches, were then compared.

The CBF values were determined using Eqs. [7] and [8]. Since five MT saturation levels were used, five CBF values were determined for each pair of control and labeled images using Eq. [8], while one CBF value was calculated using Eq. [7]. We assumed that $\lambda = 0.9$ ml/g (18). The T_1 value was obtained from inversion recovery images without any MT effects before the injection of MION. If the arterial component existed in the signal (such as images before the injection of MION), CBF values were determined using Eq. [8] with $\tau_a = \sim 0.3$ s (unpublished data with dynamic ASL method: $\sim 295.2 \pm 64.9$ ms ($N = 8$), and 0.26 s from Ref. 13). After MION is injected, the arterial blood signal contribution will be minimal. Assuming that the arterial blood volume is 1 ml/100 g ($\cong 1\%$) and blood flow is ~200 ml/100 g/min, a mean transit time of blood passing through arterial blood vessels is (1 ml/100 g)/(200 ml/100 g/min) = ~0.3 s. Thus, CBF values were obtained using Eq. [8] with $\tau_c = \sim 0.3$ s + ~0.3 s = ~0.6 s (confirmed in separate experiments under similar animal conditions). Similarly, Eq. [7] used a transit time of 0.6 s. Statistical analyses were performed using the ORIGIN 7.0 program (Microcal, Northampton, MA). The data are reported as the mean ± SD.

RESULTS

Changes in Blood Relaxation Times Due to the Contrast Agent (MION)

The T_2 of *arterial* (not venous) blood changed from 40.03 ± 1.77 to 14.13 ± 3.59 ms after 1 mg Fe/kg body weight of MION was injected ($N = 10$), resulting in $R_{2(blood)}$ of 45.8 s^{-1}. Therefore, arterial blood signals can be significantly reduced at TE = 25 ms after the MION injection. The change in T_1 of blood due to the MION injection was from 2.30 ± 0.19 to 1.14 ± 0.06 s ($N = 10$), resulting in $\Delta R_{1(blood)}$ of 0.44 s^{-1}. Our T_1 value of plasma before MION injection was similar to the T_1 of whole blood (19). The relaxation times of arterial blood before the injection of MION are consistent with those reported previously (11,19). The averaged relaxation times were used for CBVa calculation. The measured labeling efficiency values in carotid arteries with an 8-s-long RF pulse were 0.82 ± 0.01 and 0.76 ± 0.03 before and after the MION injection, respectively ($N = 3$). This is consistent with previous measurements (0.8) with a similar experimental setup (20). In our MOTIVE studies, 50% of the spin preparation duration was used for spin labeling. Thus, spin labeling efficiency was 50% relative to that of 100% duty cycle (Fig. 2b), and α_0 was 0.41 and 0.38 before and after 1 mg/kg MION injection, respectively.

Arterial Blood Volume Measurements Modulated by the Contrast Agent

We investigated the dependency of saturation duration on MT effects by varying the spin preparation period (Fig. 2c).

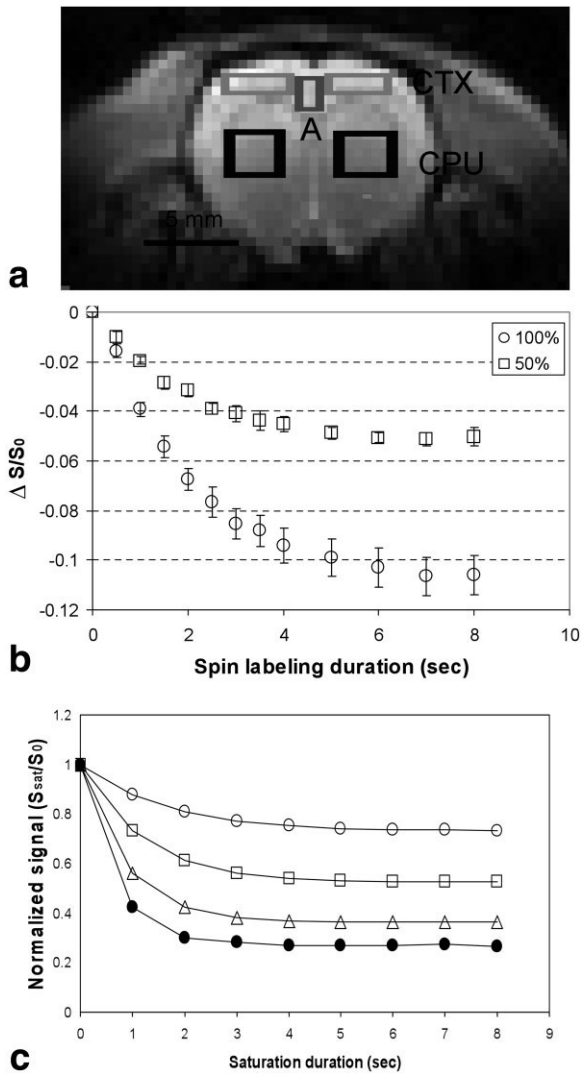

FIG. 2. Time-dependent ASL signals and MT effects achieved using the pulse sequence shown in Fig. 1. **a:** Anatomical EPI image with ROIs. The cortex (CTX) ROI consists of two rectangular boxes at the cortex. The caudate putamen (CPU) ROI is shown as two boxes in the caudate putamen. The artery ROI is included in the anterior cerebral artery (labeled A). These three ROIs were used for further analyses. **b:** Normalized ASL signal intensities ($\Delta S/S_0$) in the cortical ROI with 50% (shown in Fig. 1) and 100% spin labeling duty cycles in six animals. For 100% duty cycle, only one spin-labeling pulse without any MT-inducing pulses was applied during the entire spin preparation period. Clearly, the spin-labeling efficiency with the 50% duty cycle was 50% of that with the 100% duty cycle. Error bars: SEM. **c:** Normalized signal intensities in the cortical ROI as a function of the spin-preparation duration for one representative animal. Normalized signal intensities in the cortex at the steady-state condition with different MT saturation levels were ~0.73 (open circles), ~0.52 (open squares), ~0.36 (open triangles), and ~ 0.26 (filled circles). The 8-s saturation duration is sufficient to reach a steady-state condition.

For images without MT effects, no RF power for MT pulses was applied. Additionally, four MT saturation levels were obtained by adjusting the power of the MT-inducing RF pulses. MR signals with MT effects were initially reduced, and reached a steady-state condition when a period of saturation of macromolecules was longer than 4 s. In subsequent studies, 8 s was used to achieve a steady-state condition for both MT effects and ASL. Identical power levels of MT pulses were used for all studies in each animal.

The arterial blood volume was calculated from signals using the MOTIVE approach with MION. The data from one representative animal are shown in Fig. 3. Normalized signal intensities of the cortex ROI (shown in Fig. 2a) from data obtained with MION were fitted against those acquired without MION using Eq. [4]. From the slope and TE = 25 ms, $\Delta R_{2(\text{tissue})}$ induced by MION was found to be 0.38 s^{-1} (Fig 3a). From the slope, intercept, and $\Delta R_{2(blood)}$, the arterial blood volume was 1.4 ml/100 g tissue in the cortical ROI. Similarly, the slope and intercept were determined from MRI obtained with and without MION on a pixel-by-pixel basis. $\Delta R_{2(\text{tissue})}$ and CBVa maps were shown in Fig. 3b and c, respectively. The edge of the $\Delta R_{2(\text{tissue})}$ map has strong intensities, possibly due to the susceptibility effect of large blood vessels at the surface of the cortex (Fig. 3b); therefore, the area with high $\Delta R_{2(\text{tissue})}$ values was not included in the cortical ROI analyses. In the arterial blood volume map (Fig. 3c), the highest volume is observed at the anterior cerebral artery in the middle of the cortex (specified by an arrow). This is consistent with the notion that pixels with large arterial vessels have high CBVa. The average CBVa values were 1.1 ± 0.5, 1.3 ± 0.6, and 1.5 ± 0.8 ml/100 g tissue (N = 10 animals) in the cortex, caudate putamen, and artery ROIs, respectively. The CBVa in the artery ROI was not much higher than that in other ROIs. This is due to the partial volume effect caused by a large ROI compared to the arterial volume, and by the application of a Gaussian filter.

Arterial Blood Volume Measurement Modulated by ASL

The CBVa can also be obtained using MOTIVE with ASL. Figure 4a and b show ASL data with MT effects from the same animal presented in Fig. 3. Normalized difference signals were fitted against normalized control signals. In the cortex area, the arterial blood volume was found to be $\lambda \times \text{intercept}/(2 \times \alpha - \text{slope})$ = 1.5 ml/100 g tissue. Similarly, arterial blood volume maps of three representative animals are shown in Fig. 4b–d. In all three animals, the highest CBVa values are found in a large artery: the anterior cerebral artery (arrow) in the medial side of the cortex, and the middle cerebral artery (black circle) in the ventral edge of the brain. This is consistent with known arterial vessel structures (21). The average CBVa values obtained using Eq. [6] were 1.0 ± 0.3, 1.0 ± 0.3, and 1.7 ± 0.6 ml/100 g tissue (N = 10) in the cortex, caudate putamen, and artery ROIs, respectively.

CBVa values were measured in all 10 animals by MOTIVE approaches with MION and ASL (Fig. 5). The values from the three ROIs were plotted against each other. The arterial blood volume values measured by both methods matched well (R^2 values of 0.60, 0.82, and 0.46 in the

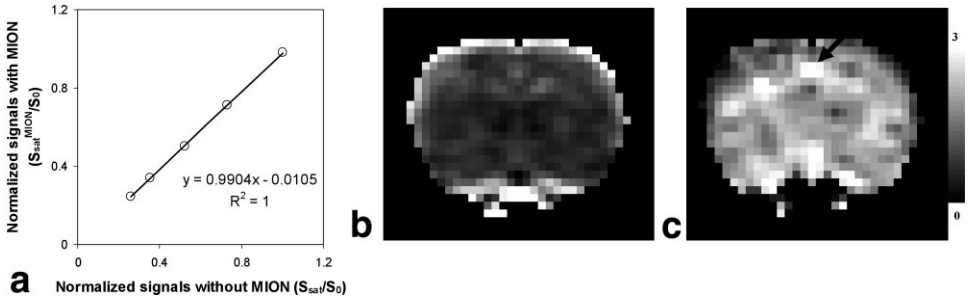

FIG. 3. Arterial blood volume calculated from data acquired before and after the injection of contrast agents with variable MT saturation levels in one representative rat. **a:** Normalized signal intensities of the cortex ROI before the injection of MION were fitted against those observed after the injection of MION at five MT saturation levels. The slope and intercept were then determined. **b:** From the slope, ΔR_2 in tissue induced by 1 mg/kg MION ($\Delta R_{2(tissue)}$ as a unit of s^{-1}) was derived on a pixel-by-pixel basis. **c:** From the intercept, slope, and in vitro ΔR_2 in blood induced by MION, an arterial blood volume map was obtained. An arrow indicates the anterior cerebral artery, which has high CBVa. For better signal averaging, arterial blood volume was calculated from the ROIs. The arterial blood volumes in one animal were 1.4 ml/100 g in the cortex area, 2.2 ml/100 g in the caudate putamen, and 2.6 ml/100 g in the artery area. Grayscale: (b) 0 – 3 s^{-1}, and (c) 0 – 3 ml/100 g.

cortex, caudate putamen, and artery area, respectively). No statistically significant differences between the two measurements were observed in the cortex ($P = 0.46$) or artery ($P = 0.19$). In the caudate putamen area, two measurements slightly differed ($P = 0.03$). Since CBVa is on an order of 1%, it is susceptible to noise, resulting in large scattering of data (especially in the arterial ROI) (Fig. 5). Since MION induced a large susceptibility gradient in a large vessel area, the arterial blood volume in the large vessel area may not be determined accurately by the contrast agent method.

Our arterial volume measurement was obtained from the linear fitting of different MT data. Errors in fitting (slope and intercept) and measurements (blood relaxation or labeling efficiency) are propagated. The determined errors of CBVa were 14%, 16%, and 14% in the cortex, caudate putamen, and artery ROIs, respectively, with the ASL method. With the contrast agent method they were 33%, 56%, and 30% in the cortex, caudate putamen, and artery ROIs, respectively.

Overestimation of CBF Caused by Arterial Blood Volume Contribution

Figure 6 shows CBF maps determined from the data from one representative animal, which were obtained with graded MT saturation levels without (a–c) and with MION (d–f). The quantitative MT dependence of calculated CBF values obtained in three ROIs for all 10 animals is plotted in Fig. 7. Clearly, CBF values calculated from ASL data

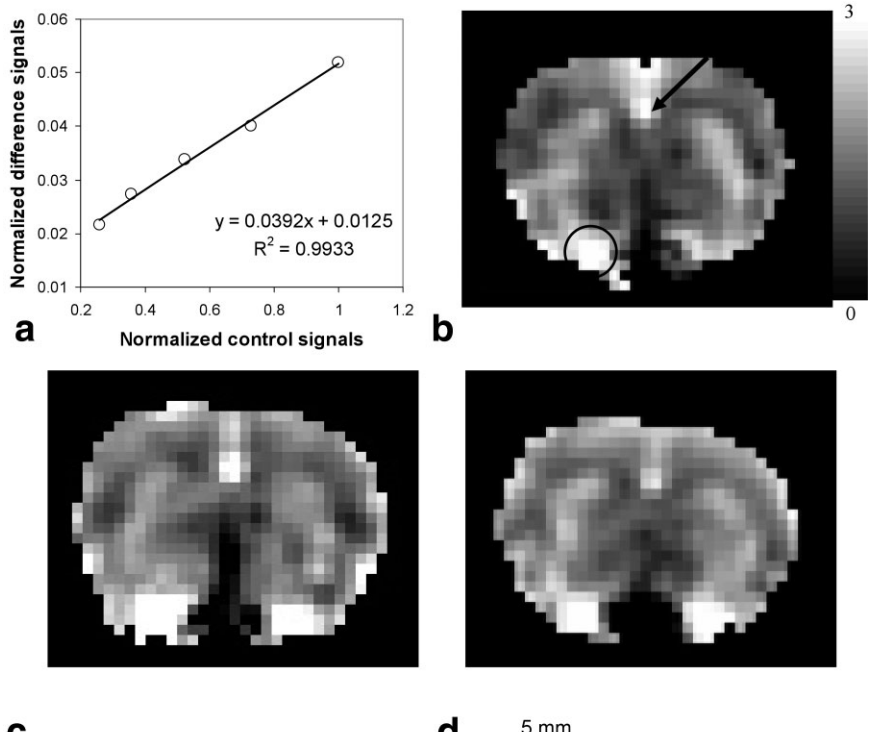

FIG. 4. Arterial blood volume determined from ASL data with various MT saturation levels in three animals. **a** and **b:** Data from the same animal shown in Fig. 3. To determine arterial blood volume, ASL data with MT effects ($\Delta S_{sat}/S_0$) were fitted against corresponding control data (S_{sat}/S_0). Cortical ROI data were plotted in a. From the intercept and the slope (see Theory section), arterial blood volume (b–**d**) was calculated on a pixel-by-pixel basis. Grayscale: 0–3 ml/100 g. An arrow indicates the anterior cerebral artery in the middle of the two hemispheres, and a black circle indicates the middle cerebral artery (b). Similar patterns were observed in all three CBVa maps. The ROI analysis of arterial blood volume revealed values of 1.5, 1.5, and 2.9 ml/100 g in the cortex, caudate putamen, and artery areas, respectively, in one animal (shown in Fig. 3).

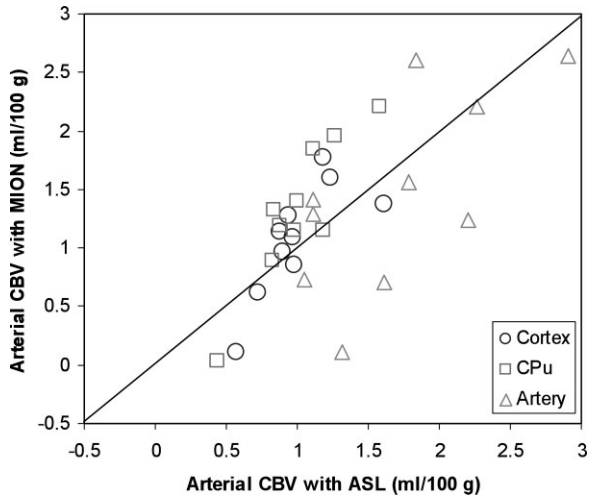

FIG. 5. Comparison of arterial blood volumes of the cortex (circles), caudate putamen (squares), and artery (triangles) ROIs measured by two MOTIVE approaches in 10 animals. Each data point represents the data from one animal. A line of identity is shown. R^2 values were 0.60, 0.82, and 0.46 in the cortex, caudate putamen, and artery areas, respectively.

without the removal of arterial blood signal (Fig. 6a and b) were dependent on MT saturation levels. At the normalized signal level (S_{sat}/S_0) of 0.26, the calculated CBF in the cortex was overestimated by 46% compared to that with no MT effect (filled symbols in Fig. 7). Similarly, the contamination of the vascular component was 32% and 56% overestimated at the normalized signal of $0.32S_0$ and $0.28S_0$ in the caudate putamen and artery area, respectively. When contribution of arterial blood signals was removed by injection of a contrast agent (Fig. 6d and e, and open symbols in Fig. 7), MT dependence of CBF quantification was eliminated. Alternatively, when tissue signal was separated from blood signal using the MOTIVE approach, the perfusion maps obtained before and after the injection of MION were similar (see Fig. 6c and f). After the arterial blood contribution was separated from the tissue signal, the CBF values calculated with MOTIVE using Eq. [7] were 194 ± 34, 222 ± 29, and 217 ± 41 ml/100 g/min in the cortex, caudate putamen, and artery areas, respectively, before the MION injection. After the MION injection, they were 176 ± 34, 216 ± 43, and 218 ± 43 ml/100 g/min in the cortex, caudate putamen, and artery areas, respectively. The difference between the two measurements was not statistically significant for each ROI ($P = 0.22$ in the cortex; $P = 0.66$ in the caudate putamen; and $P = 0.96$ in the artery).

DISCUSSION

In Vivo Measurements of Arterial Blood Volume

Arterial blood volumes were determined by two independent MOTIVE approaches: ASL and contrast agent. The arterial blood volumes in rats were consistent (1.0 ml/100 g vs. 1.1 ml/100 g in the cortex, and 1.0 ml/100 g vs. 1.3 ml/100 g in the caudate putamen), suggesting that our MRI approaches are robust. The arterial blood volumes (1.0–1.3 ml/100 g) in our studies agree with those observed by Ito et al. (22) in humans (1.1% ± 0.4%). In their study a dynamic blood and tissue compartment model was used in conjunction with $C^{15}O$ and time-dependent $H_2^{15}O$ PET studies.

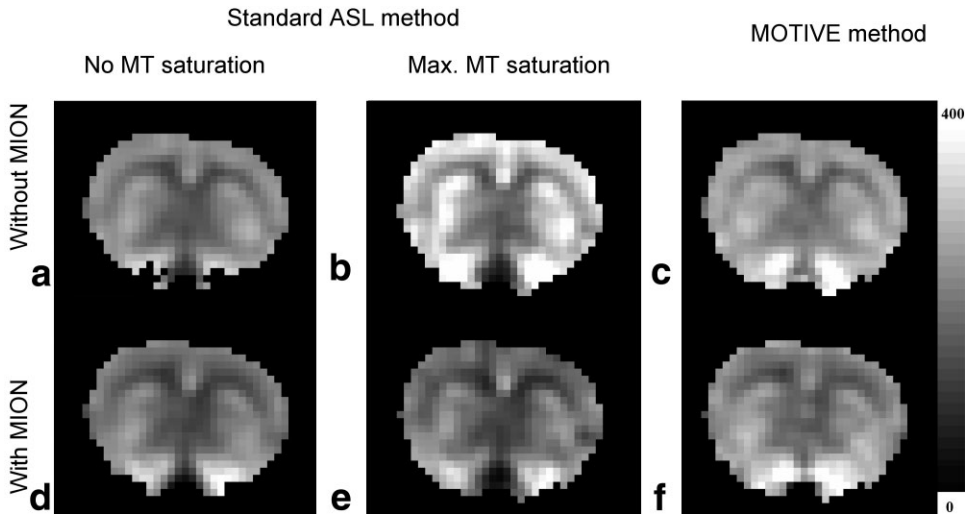

FIG. 6. CBF maps (as units of ml/100 g tissue/min) obtained without (**a–c**) and with (**d–f**) a contrast agent in a representative animal. The normalized signal intensities (S_{sat}/S_0) in the cortex area were (a and d) 1.0 (i.e., no MT effects), and (b and e) 0.27. CBF values were calculated from ASL data with each MT saturation level using the conventional single-compartment model (a, b, d, and e), and from all data with five MT saturation levels (c and f). a and b: Before the injection of MION, the calculated CBF values increased with the MT saturation levels, suggesting that vascular signal was emphasized. d and e: However, after the intravascular signal was reduced by MION injection, the calculated CBF remained constant. Similarly, the intravascular contribution can be separated from the ASL data before the injection of MION. The CBF maps (c: before MION injection; f: after MION injection) obtained using Eq. [7] matched extremely well. This suggests that calculated CBF values are overestimated when the one-coil CASL method with a large MT effect is used without suppression of the intravascular contribution. Grayscale bar: 0–400 ml/100 g/min.

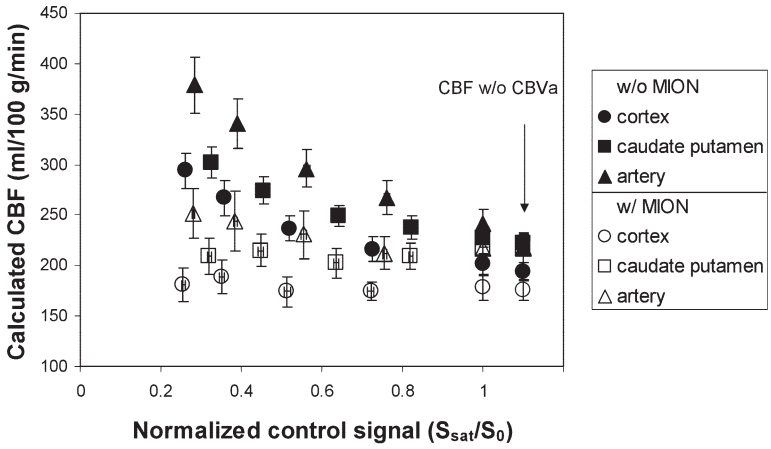

S_{sat}/S_0 (cortex)	1	0.72	0.51	0.35	0.26	w/o CBVa
CBF (ml/100 g/min)	210 ± 33	216 ± 38	236 ± 38	266 ± 53	293 ± 54	194 ± 34
p - value	0.03949	0.00032	0.00003	0.00008	0.00001	

FIG. 7. Dependence of MT effects on calculated CBF values without (filled symbols) and with (open symbols) the suppression of intravascular signals with MION (N = 10). In each animal, cortex (circle), caudate putamen (square), and artery (triangle) ROIs were used. At each MT saturation level, CBF values determined using the conventional single-compartment model (Eq. [8]) were plotted as a function of normalized control signal intensities (S_{sat}/S_0). For comparison, CBF values were determined by Eq. [7] to remove the arterial blood contribution (marked as CBF without CBVa at the *x*-axis value of ~1.1). After MION injection (open symbols), the calculated CBF was independent of the MT saturation levels. The difference between the calculated CBF at different MT saturation levels before the MION injection can be explained by different proportions of the vascular contributions. Error bars: SEM. The table inserted below the figure provides CBF values of the cortex ROI obtained before the MION injection as a function of normalized signal intensities. The CBF value calculated using the single-compartment model was compared with that determined by the MOTIVE method. Its statistical *P*-value is shown in the table.

Potential error in our CBVa measurements may result from the assumption of a negligible venous CBV contribution. In ASL methods, labeled blood spins travel into capillaries, exchange with tissue water, and finally exit to the veins. Labeled spins will eventually recover to full magnetization M_0 due to T_1 relaxation during the travel time, and thus venous blood contribution is minimal. Consequently, our assumption of a negligible venous blood contribution is reasonable. However, in the contrast agent method, venous blood contribution is dependent on the R_2 of venous blood ($R_{2(\mathrm{vein})}$), and TE. When signal from the venous blood volume is included, the second term of Eq. [4] should be replaced with

$$[(\nu_a \cdot e^{-R_{2(\mathrm{artery})}TE} + \nu_v \cdot e^{-R_{2(\mathrm{vein})}TE})/e^{-R_{2(\mathrm{tissue})}TE}](e^{-\Delta R_{2(\mathrm{blood})}TE} - e^{-\Delta R_{2(\mathrm{tissue})}TE}). \quad [9]$$

Assuming that ν_v is 3 times ν_a, the arterial blood volume measured at 9.4T is overestimated by 4% at TE = 25 ms when $R_{2(\mathrm{vein})}$ is 200 s^{-1}, and by 18% when $R_{2(\mathrm{vein})}$ is 143 s^{-1}. This venous volume contribution may cause a higher CBVa with the contrast agent method (Fig. 5). Equation [9] assumed that the venous blood magnetization is M_0, which is similar to the arterial blood magnetization in Eq. [2]. However, the saturated longitudinal spins in tissue exchange with capillary spins. Then exchanged spins drain into the venous blood pool with T_1 relaxation during the transit time. Thus, the magnetization of venous blood will not be M_0, which will induce errors in the CBVa determination. At low magnetic fields, the R_2's of arterial blood and tissue differ, and the contribution of venous signal is not negligible. The arterial and venous blood volumes may be evaluated by weighting arterial and venous signal contributions differently. At a long TE (especially with a gradient-echo sequence), signals from the venous pool can be minimized. Thus, the arterial blood volume can be measured. Both arterial and venous signals contribute significantly at short TE and/or low magnetic fields. With knowledge of the arterial blood volume and relaxation parameters, the venous blood volume can be determined.

Both MOTIVE approaches can be used to measure arterial blood volume. ASL measurements can be repeated in the same subject, but the contrast agent method cannot be repeated. Thus the ASL methods can provide higher SNR. Pulsed ASL methods can be adapted for the measurement of arterial blood volume. During the spin labeling time (e.g., TI), different MT saturation levels can be generated by saturating macromolecules using long pulse(s). Then, by using Eq. [6] with minor modifications, arterial blood volume and blood flow can be simultaneously determined by incorporating the loss of labeled spins during the spin labeling time.

The main idea behind the MOTIVE approach is that tissue signal is separated from blood by MT effects. The separation of tissue and blood signals can also be carried out with the use of flow-crushing gradients. However, the MOTIVE approach can modulate tissue and blood signals independently, while the simple bipolar approach modu-

lates only blood signals. Multiple levels of tissue signal intensity can be achieved in the MOTIVE approach, while only two points (with and without crushing arterial vessel signals) can be obtained in the bipolar method. The advantage of the MOTIVE technique is that is offers a large dynamic range, because five different MT saturation levels (or even more points) are used. Therefore, the MOTIVE method is more accurate for separating tissue and blood than the simpler two-point approach. The disadvantages of MOTIVE are a long measurement time and RF deposition caused by MT-inducing pulses.

Quantification of CBF

According to CBF models (23), the cross-relaxation constant (δ) between water and macromolecules is an important factor in determining CBF values. When macromolecules are saturated, δ will be zero; thus, in the one-coil ASL method, δ is not included. In the two-coil system without the saturation of macromolecules, Zhang et al. (23) reported that ignoring δ would cause an approximately 17% underestimation of CBF at 4.7T. In our 9.4T studies, when blood signal contribution was minimized after the injection of MION, the calculated CBF value without considering δ was independent of MT saturation levels. This suggests that CBF quantification does not need to include δ, which is $k_{for}/(1 + k_{rev}T_{1m})$ where k_{for} and k_{rev} are the MT rates, and T_{1m} is the spin-lattice relaxation time of the macromolecular spins. Since T_{1m} increases as the magnetic field increases (24), δ may be negligible at 9.4T.

In ASL studies without the suppression of intravascular signals, CBF values can be overestimated. In the one-coil ASL method, MT effect reduces tissue signals by about 70% (23). In this condition, CBF values determined without the suppression of intravascular signals can be overestimated by about ~50% at 9.4T. Based on previous one-coil ASL measurements without suppression of arterial blood contribution at 4.7T, cortical CBF values of isoflurane-anesthetized rats were found to be 426 ml/100 g/min and 387 ml/100 g/min (13,25,26). These values are much higher than our CBF value. The overestimation of previous CBF measurements can be easily explained by the contamination of arterial blood signals. It is important to remove the arterial blood volume contribution to accurately quantify CBF when the MT effect is significant. Several methods can be used for this purpose. First, the bipolar gradient can remove the contribution of inverted spins in large arterial vessel components (15). It has been reported that a *b*-value of 30 s/mm^2 can eliminate signals from most of the fast-moving arterial blood (5,11). Second, a post-labeling delay time can be used (27). Unlabeled spins fill up an arterial vascular system during the post-labeling delay time (*w*), which minimizes the contribution of arterial blood to ASL signals. This method requires a reasonably accurate post-labeling delay time because a too-short *w* will not remove signals from arterial vessels, and a too-long *w* will result in the loss of perfusion sensitivity. Third, the MOTIVE method can separate tissue signals from blood signals. If the pixels contain multiple tissue types (such as gray and white matter) with different R_2 values and MT levels, the calculated CBF values will have errors. In our measurements, the ROI with mostly gray matter had relatively homogeneous MT saturation levels (data not shown), and thus we do not expect any significant errors in CBF quantification.

Our CBF values in the rat brain obtained from ASL data with the removal of the arterial contribution using graded MT saturation levels are similar to CBF values obtained under isoflurane anesthesia determined by the ^{14}C-iodoantipyrine autoradiography method (i.e., 154 ± 19 ml/100 g/min in the cortex) (28). Recently reported CBF values obtained using the two-coil system without MT effects (29) agree well with our CBF values. (As a side note, Tsekos et al. (19) reported that their CBF measurements obtained by FAIR (without MT effects) in rats at 9.4T agreed with those obtained by iodoantipyrine autoradiography under the same anesthesia).

To accurately quantify CBF, any arterial volume contribution must be eliminated. Once the contribution of arterial blood volume is removed, the spin labeling efficiency should then be determined by τ_c (not τ_a). In our ASL measurements without MT effects (such as in two-coil ASL or FAIR), CBF values quantified with and without suppression of arterial blood volume agreed extremely well (see Fig. 7). This finding can be explained by two competing mechanisms, i.e., the contamination of the arterial volume is coincidentally compensated by the overestimation of labeling efficiency ($\tau_a < \tau_c$). To further investigate this issue, we simulated the effect of the arterial blood volume contribution on the quantification of CBF with values for humans at 1.5T (CBF = 60 ml/100 g/min, blood T_1 = 1.2 s (14), and τ_a = 0.8 s (30)) and for rats at 9.4T (CBF = ~200 ml/100 g/min, blood T_1 = 2.3 s, and τ_a = 0.3 s). We found that the compensatory mechanism works reasonably well (i.e., the effect of ignoring the contribution of arterial volume is canceled by also ignoring the difference between τ_a and τ_c if CBVa = ≤1%). Therefore, CBF measurements can be performed (with high sensitivity) without the suppression of arterial blood vessels, and quantification will not be compromised when CBVa ≤ 1%.

CONCLUSIONS

We developed novel MRI methods to determine CBVa and CBF. The arterial blood volume can be obtained by modulating tissue signals by MT effects, and by changing blood signals by the injection of contrast agents. By using ASL methods with graded MT saturation levels, the CBF and arterial blood volume can be simultaneously obtained. This method is also applicable to humans. The proposed technique allows high-resolution imaging, and thus may shed light on physiological and pathological changes in normal and diseased brains. For example, the arterial blood volume measurement could help resolve the controversy over whether venous or arterial vessels dilate during neural activation.

ACKNOWLEDGMENTS

We thank Kamil Ugurbil of the University of Minnesota for continuing support of this project, Kristy Hendrich for helpful discussions, and Michelle Tasker for careful proofreading of this manuscript.

REFERENCES

1. Rosen BR, Belliveau JW, Vevea JM, Brady TJ. Perfusion imaging with NMR contrast agents. Magn Reson Med 1990;14:249–265.
2. Calamante F, Thomas DL, Pell GS, Wiersma J, Turner R. Measuring cerebral blood flow using magnetic resonance imaging techniques. J Cereb Blood Flow Metab 1999;19:701–735.
3. Zaharchuk G, Bogdanov Jr AA, Marota JJ, Shimizu-Sasamata M, Weisskoff RM, Kwong KK, Jenkins BG, Weissleder R, Rosen BR. Continuous assessment of perfusion by tagging including volume and water extraction (CAPTIVE): a steady-state contrast agent technique for measuring blood flow, relative blood volume fraction, and the water extraction fraction. Magn Reson Med 1998;40:666–678.
4. Thomas DL, Lythgoe MF, Calamante F, Gadian DG, Ordidge RJ. Simultaneous noninvasive measurement of CBF and CBV using double-echo FAIR (DEFAIR). Magn Reson Med 2001;45:853–863.
5. Duong TQ, Kim SG. In vivo MR measurements of regional arterial and venous blood volume fractions in intact rat brain. Magn Reson Med 2000;43:393–402.
6. Detre JA, Leigh JS, Williams DS, Koretsky AP. Perfusion imaging. Magn Reson Med 1992;23:37–45.
7. Balaban RS, Chesnick S, Hedges K, Samaha F, Heineman FW. Magnetization transfer contrast in MR imaging of the heart. Radiology 1991; 180:671–675.
8. Wolff SD, Balaban RS. Magnetization transfer contrast (MTC) and tissue water proton relaxation in vivo. Magn Reson Med 1989;10:135–144.
9. Grubb Jr RL, Raichle ME, Eichling JO, Ter-Pogossian MM. The effects of changes in $PaCO_2$ on cerebral blood volume, blood flow, and vascular mean transit time. Stroke 1974;5:630–639.
10. Leenders KL, Perani D, Lammertsma AA, Heather JD, Buckingham P, Healy MJ, Gibbs JM, Wise RJ, Hatazawa J, Herold S, Beaney RP, Brooks DJ, Spinks T, Rhodes C, Frackowiak RSJ, Jones T. Cerebral blood flow, blood volume and oxygen utilization. Normal values and effect of age. Brain 1990;113(Pt 1):27–47.
11. Lee SP, Silva AC, Ugurbil K, Kim SG. Diffusion-weighted spin-echo fMRI at 9.4 T: microvascular/tissue contribution to BOLD signal changes. Magn Reson Med 1999;42:919–928.
12. Orrison WW, Lewine JD, Sanders JA, Hartshorne MF. Functional magnetic resonance imaging. Functional brain imaging. St. Louis: Mosby; 1995.
13. Barbier EL, Silva AC, Kim SG, Koretsky AP. Perfusion imaging using dynamic arterial spin labeling (DASL). Magn Reson Med 2001;45: 1021–1029.
14. Ye FQ, Mattay VS, Jezzard P, Frank JA, Weinberger DR, McLaughlin AC. Correction for vascular artifacts in cerebral blood flow values measured by using arterial spin tagging techniques. Magn Reson Med 1997;37:226–235.
15. Silva AC, Zhang W, Williams DS, Koretsky AP. Estimation of water extraction fractions in rat brain using magnetic resonance measurement of perfusion with arterial spin labeling. Magn Reson Med 1997;37:58–68.
16. Silva AC, Zhang W, Williams DS, Koretsky AP. Multi-slice MRI of rat brain perfusion during amphetamine stimulation using arterial spin labeling. Magn Reson Med 1995;33:209–214.
17. Zhang W, Williams DS, Koretsky AP. Measurement of rat brain perfusion by NMR using spin labeling of arterial water: in vivo determination of the degree of spin labeling. Magn Reson Med 1993;29:416–421.
18. Herscovitch P, Raichle ME. What is the correct value for the brain–blood partition coefficient for water? J Cereb Blood Flow Metab 1985; 5:65–69.
19. Tsekos NV, Zhang F, Merkle H, Nagayama M, Iadecola C, Kim SG. Quantitative measurements of cerebral blood flow in rats using the FAIR technique: correlation with previous iodoantipyrine autoradiographic studies. Magn Reson Med 1998;39:564–573.
20. Silva AC, Kim SG. Pseudo-continuous arterial spin labeling technique for measuring CBF dynamics with high temporal resolution. Magn Reson Med 1999;42:425–429.
21. Paxinos G. The rat nervous system. 2nd edition. San Diego: Academic Press; 1995.
22. Ito H, Kanno I, Iida H, Hatazawa J, Shimosegawa E, Tamura H, Okudera T. Arterial fraction of cerebral blood volume in humans measured by positron emission tomography. Ann Nucl Med 2001;15:111–116.
23. Zhang W, Silva AC, Williams DS, Koretsky AP. NMR measurement of perfusion using arterial spin labeling without saturation of macromolecular spins. Magn Reson Med 1995;33:370–376.
24. Ceckler TL, Balaban RS. Field dispersion in water-macromolecular proton magnetization transfer. J Magn Reson B 1994;105:242–248.
25. Hendrich KS, Kochanek PM, Williams DS, Schiding JK, Marion DW, Ho C. Early perfusion after controlled cortical impact in rats: quantification by arterial spin-labeled MRI and the influence of spin-lattice relaxation time heterogeneity. Magn Reson Med 1999;42:673–681.
26. Hendrich KS, Kochanek PM, Melick JA, Schiding JK, Statler KD, Williams DS, Marion DW, Ho C. Cerebral perfusion during anesthesia with fentanyl, isoflurane, or pentobarbital in normal rats studied by arterial spin-labeled MRI. Magn Reson Med 2001;46:202–206.
27. Alsop DC, Detre JA. Reduced transit-time sensitivity in noninvasive magnetic resonance imaging of human cerebral blood flow. J Cereb Blood Flow Metab 1996;16:1236–1249.
28. Hansen TD, Warner DS, Todd MM, Vust LJ, Trawick DC. Distribution of cerebral blood flow during halothane versus isoflurane anesthesia in rats. Anesthesiology 1988;69:332–337.
29. Sicard K, Shen Q, Brevard ME, Sullivan R, Ferris CF, King JA, Duong TQ. Regional cerebral blood flow and BOLD responses in conscious and anesthetized rats under basal and hypercapnic conditions: implications for functional MRI studies. J Cereb Blood Flow Metab 2003;23: 472–481.
30. Wong EC, Luh WM, Liu TT. Turbo ASL: arterial spin labeling with higher SNR and temporal resolution. Magn Reson Med 2000;44:511–515.